Journal of Southeast University (English Edition) Vol. 37, No. 3, pp. 264 - 271 Sept. 2021 ISSN 1003—7985

Influence of micro asperity contact and radial clearance on the tribological properties of crankpin bearings

Nguyen Van Liem[1,2,3] Zhang Jianrun[1] Huang Dacheng[1]

([1]School of Mechanical Engineering, Southeast University, Nanjing 211189, China)
([2]School of Mechanical and Electrical Engineering, Hubei Polytechnic University, Huangshi 435003, China)
([3]Key Laboratory of Intelligent Conveying Technology and Device, Hubei Polytechnic University, Huangshi 435003, China)

Abstract: A new hybrid numerical method that couples the dynamic slider-crank mechanism (SCM) and crankpin bearing (CB) lubrication models is proposed to analyze the effect of micro asperity contact on the tribological properties of a CB. In the hybrid model, the dynamic equations of the SCM are established based on the Newton method, while the lubrication equations of the CB are established on the basis of the Reynolds equation. Experimental data of the engine are also used in simulation analyses to enhance the reliability of the results. The load-bearing capacity (LBC) and friction force of the CB are selected as objective functions. Results show that the LBC has a negligible effect on the tribological properties of the CB, but the friction force greatly affects the resistance of the bearing under different radial clearances and surface roughness values. In particular, the maximum friction force in the asperity contact region accounts for 40.5% of the maximum total friction force at a radial clearance of 5 μm and 77.7% of the maximum total friction of the CB with a surface roughness of 10 μm.

Key words: crankpin bearing; tribological property; slider-crank mechanism; asperity contact

DOI: 10.3969/j.issn.1003 - 7985.2021.03.005

Improving power and reducing friction loss are key concerns in the design and research of internal combustion engines. Therefore, research on the friction and lubrication performance of bearings is essential to optimize the design parameters of engines.

A large number of studies have been conducted over the last few decades to assess the influence of various piston design parameters on the performance of combustion engines. For example, the inertial force of the piston and the eccentricity between the crankshaft and cylinder center have been investigated to reduce the horizontal impact force of the piston on the cylinder bore and engine balance[1-3]. The influence of the friction force generated by the piston skirt and ring against the cylinder bore during movement, as well as that of the relative motion of the joints of the slider-crank mechanism (SCM) on the engine power, has also been analyzed[4-6]. The results obtained show that the friction power loss caused by relative motion between the friction pairs is not negligible. Research on methods to improve lubrication between the piston and cylinder[2, 6-7] and simulation of the lubrication models of crankshaft bearings[4, 8] to reduce the friction power loss in the SCM has been performed. The results of these works reveal that friction power losses are significantly reduced by increasing the oil film thickness and become stable on lubricated surfaces.

The lubrication condition of journal bearings often belongs to the mixed-or starved-lubrication regime when the sliding pairs are at the start/end verge or in an overloaded state[9-10]. In this case, the micro asperity contact in the mixed-lubrication regime of the journal bearing would increase the friction and wear at the contact region between the shaft and bearing surfaces[11-12]. Thus, investigating the effect of the surface roughness of the journal bearings on the lubrication performance of a bearing under both hydrodynamic and mixed lubrication conditions is necessary.

Previous research[7, 13] suggested that micro asperity contact with a rough surface exerts a great influence on the lubrication performance of journal bearings. Although some scholars have investigated the effects of the pressure[9-10] and shear stress[7, 14] of the asperity contact on the load-bearing capacity (LBC) and friction force of journal bearings, the effects of the LBC and friction force on the tribological properties of journal bearings in the mixed-lubrication regime have not yet been clarified. Moreover, the aforementioned studies mainly considered the effect of static load and usually ignored the external load acting on the journal bearings[10, 15]. The asperity contact load is known to be directly correlated with the wear profile of the bearing bore and the load carried by surface asperities. During the working cycle of an en-

Received 2020-11-01, **Revised** 2021-06-10.

Biographies: Nguyen Van Liem (1986—), male, doctor; Zhang Jianrun (corresponding author), male, doctor, professor, zhangjr@seu.edu.cn.

Foundation items: The National Key Research and Development Project (No. 2019YFB2006402), the Open Fund Project of Key Laboratory of Intelligent Conveying Technology and Device, Hubei Polytechnic University.

Citation: Nguyen Van Liem, Zhang Jianrun, Huang Dacheng. Influence of micro asperity contact and radial clearance on the tribological properties of crankpin bearings [J]. Journal of Southeast University (English Edition), 2021, 37(3): 264 - 271. DOI: 10.3969/j.issn.1003 - 7985.2021.03.005.

gine, the dynamic load acting on the crankpin bearing (CB) may rapidly change in terms of direction and intensity under changing speeds[4-5]. These phenomena, to some extent, may aggravate the influence of the micro asperity contact in the mixed-lubrication regime on the tribological properties of the CB and increase the power loss of the engine.

The current paper presents a new numerical simulation method that combines the dynamic SCM and CB lubrication models to evaluate the tribological properties of a CB comprehensively. In contrast to previous studies that only considered LBC and the friction force of the oil film on the tribological properties of the CB, this work completely analyzes the influence of the micro asperity contact and radial clearance on these properties. A program written in MATLAB is then applied to solve the corresponding dynamic and lubrication equations. Various radial clearances and surface roughness values are considered in the mixed-lubrication regime to explain their influence on the tribological properties of CBs.

1 Method

1.1 Dynamic slider-crank-mechanism model

The dynamic force of the SCM model is calculated by assuming that the center of the crankshaft coincides with the cylinder center, as shown in Fig. 1.

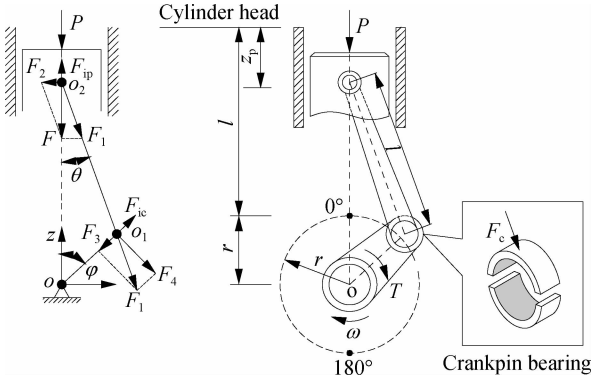

Fig. 1 SCM model with lubricated joints

According to the SCM model and its dynamic motion principle, the piston's acceleration in the z-direction can be determined by[7, 15]

$$\ddot{z}_p = r\omega^2(\cos\varphi + \lambda\cos 2\varphi) \tag{1}$$

where $\lambda = r/l$; r and ω are the rotational radius and angular velocity of the crankshaft, respectively; and l is the connecting rod length.

Assuming that the mass of the connecting rod is the sum of the masses of the large-rod end (m_{br}) at o_1 and the small-rod end (m_{sr}) at o_2, the inertial force of the total mass of the piston (m_p) and the small-rod end is determined by

$$F_{ip} = -\ddot{m}z_p = -(m_p + m_{sr})r\omega^2(\cos\varphi + \lambda\cos 2\varphi) \tag{2}$$

When a combustion gas pressure is exerted on the piston peak ($P = p_g\pi R^2$), the forces acting on the connecting rod, cylinder wall, and crankshaft can be expressed as follows:

$$\left.\begin{aligned} F_1 &= \frac{F}{\cos\theta} = \frac{P + F_{ip}}{\cos\theta} \\ F_2 &= F\tan\theta = \frac{P + F_{ip}}{\tan\theta} \\ F_3 &= F_1\cos(\varphi + \theta) \\ F_4 &= F_1\sin(\varphi + \theta) \end{aligned}\right\} \tag{3}$$

The total mass of the large-rod end of the connecting rod is rotated with an angular velocity of the crankshaft, and the centrifugal inertial force on the rod is written as follows:

$$F_{ic} = -m_{br}r\omega^2 \tag{4}$$

The bearing of the connecting rod provides the crankpin with a rotating motion within the rod. Thus, the total force acting on the CB is

$$F_c = \sqrt{(F_{ic} + F_3)^2 + F_4^2} \tag{5}$$

Changes in force F_c in terms of direction and intensity are then used as the dynamic load to analyze the tribological properties of the CB.

1.2 Crankpin bearing lubrication model

The CB is impacted by the dynamic force F_c and rotated with the same angular velocity ω of the crankshaft. A journal bearing consisting of the shaft imposed by the external dynamic load $W_0 = F_c$ and rotating inside the bearing with the angular velocity ω is modeled to analyze the tribological properties of the CB; the Cartesian counterpart of this model is also constructed[16], as plotted in Fig. 2(a). The surface roughness of the shaft and bearing, which has a great influence on the impact force between the shaft and bearing[11], and the lubrication performance of the journal bearings[10, 15] are further considered in this model, as shown in Fig. 2(b).

In Figs. 2(a) and (b), r_b and r_s refer to the bearing and shaft radius ($r_b > r_s$), respectively, and the small gap between the bearing and shaft is filled with lubricating oil to generate hydrodynamic pressure. Moreover, e is the eccentricity between the center of the shaft and the bearing; $u_0 = \omega r_b$ refers to the relative sliding velocity between the shaft and bearing surfaces; ψ and φ are the attitude angle and angular coordinate, respectively, B is the bearing width; and h and p are the oil film thickness and pressure, respectively. Here h is determined by the relative position between the shaft and bearing and could be expressed as follows[10, 12]:

$$h = r_b - r_s + e\cos\varphi = c(1 + \varepsilon\cos\varphi) \tag{6}$$

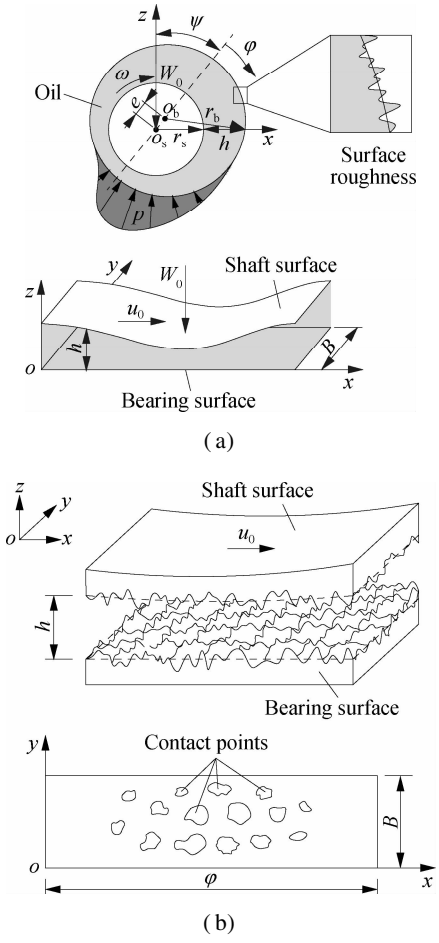

Fig. 2 Impact forces on the CB under various angular speeds. (a) Lubrication model; (b) Surface roughness and contact model

where $c = r_b - r_s$ and $\varepsilon = e/c$ are the radial clearance and eccentricity ratio between shaft and bearing $(0 < \varepsilon < 1)$, respectively.

According to the model in Fig. 2(a), the bearing surface is fixed in the x-and y-directions, while the shaft surface only moves in the x-direction under some velocity u_0. Thus, the velocity boundary conditions on the CB surfaces can be expressed as

$$\left.\begin{aligned} u\,|_{z=0} &= 0 \quad \text{at the bearing surface} \\ u\,|_{z=h} &= u_0 \quad \text{at the shaft surface} \end{aligned}\right\} \tag{7}$$

The lubrication equation of the CB can be conveniently solved by assuming that the influence of the inertia of the lubricant flow is negligible, that the lubricant density and viscosity are constant in the working process, and that the fluid velocity in the z-direction is equal to zero. In practical conditions, however, the CB surfaces are randomly oriented, as shown in Fig. 2(b). Thus, the pressure-flow factors of φ_x and φ_y reflect the resistance of the surface roughness to the lubricant flow[15], and the shear flow factor φ_s of the additional flow attributed to these two factors[13] may be employed to determine the expected volumetric flow.

According to the fluid continuity condition, the Reynolds equation of the expected volumetric flow is determined by[15, 17]

$$\frac{\partial}{\partial x}\left(\varphi_x h^3 \frac{\partial p}{\partial x}\right) + \frac{\partial}{\partial y}\left(\varphi_y h^3 \frac{\partial p}{\partial y}\right) = 6\eta u_0 \left(\frac{\partial h}{\partial x} + \sigma \frac{\partial \varphi_s}{\partial x}\right) + 12\eta \frac{\partial h}{\partial t} \tag{8}$$

where σ is the variance of the composite surface roughness of the CB and η is the dynamic viscosity of the oil.

The dimensionless form of Eq. (8) is expressed as

$$\beta^2 \frac{\partial}{\partial \varphi}\left(\varphi_x H^3 \frac{\partial P}{\partial \varphi}\right) + \frac{\partial}{\partial Y}\left(\varphi_y H^3 \frac{\partial P}{\partial Y}\right) = \Lambda_1 \left(\frac{\partial H}{\partial \varphi} + \Gamma \frac{\partial \varphi_s}{\partial \varphi}\right) + \Lambda_2 \frac{\partial H}{\partial T} \tag{9}$$

where $\varphi = x/r_b$, $Y = y/B$, $H = h/c$, $P = p/p_0$, $T = t/t_0$, $u_0 = \omega r_b$, $\Lambda_1 = 6\eta\omega B^2/(p_0 c^2)$, $\Lambda_2 = 12\eta B^2/(t_0 p_0 c^2)$, $\beta = B/r_b$, $\Gamma = \sigma/c$, and $p_0 = 101\ 325$ Pa is the standard atmospheric pressure.

Eq. (9) can be solved by determining the boundary conditions of the oil film pressure. Assuming that an oil film thickness is distributed on the CB, the inlet/outlet of the lubricant is located at the point at which the maximum film thickness corresponds to $\varphi = 0°$ and $360°$. The atmospheric pressure p_0 is the ambient pressure around the CB and the inlet/outlet pressure for the computational domain. Thus, the pressure boundary conditions are defined by

$$\left.\begin{aligned} p\,|_{\varphi=0^\circ} &= p\,|_{\varphi=360^\circ} \\ p\,|_{y=0} &= p\,|_{y=B} = 0 \end{aligned}\right\} \tag{10}$$

1.3 Mixed hydrodynamic lubrication forces

1.3.1 Load bearing capacity

Under the effect of W_0, the LBC generated by the oil film pressure is expressed as[18]

$$W_{of} = \sqrt{\left(-\iint p\cos\varphi \mathrm{d}x\mathrm{d}y\right)^2 + \left(-\iint p\sin\varphi \mathrm{d}x\mathrm{d}y\right)^2} \tag{11}$$

In addition, in the mixed-lubrication regime of the contact between the shaft and the bearing surfaces, the asperity contact pressure p_{ac} greatly influences the LBC when the ratio of the oil film thickness $h/\sigma < 4$[12]. Assuming that the surface roughness obeys a Gaussian distribution, p_{ac} can be calculated according to the asperity contact model of Greenwood and Tripp as follows[9]:

$$p_{ac} = \frac{16\sqrt{2}\,\pi(\zeta\eta\sigma)^2 E^*}{15}\sqrt{\frac{\sigma}{\zeta}} F_{5/2}\left(4 - \frac{h}{\sigma}\right) \tag{12}$$

where E^* is the composite elastic modulus; ζ is the asperity radius of curvature; and $F_{5/2}(4 - h/\sigma)$ is the probabil-

ity of the asperity height of the surface roughness.

Thus, the LBC generated by the p_{ac} can be expressed as

$$W_{ac} = \sqrt{\left(-\iint p_{ac}\cos\varphi \mathrm{d}x\mathrm{d}y\right)^2 + \left(-\iint p_{ac}\sin\varphi \mathrm{d}x\mathrm{d}y\right)^2} \tag{13}$$

Based on the LBC of the W_{of} and W_{ac}, the actual LBC of the CB is then determined as follows:

$$W_b = \sqrt{W_{of}^2 + W_{ac}^2} \tag{14}$$

where W_b is equal to the external dynamic load acting on the CB, as written in Eq. (5).

1.3.2 Friction force and friction coefficient

Under the effect of interfacial shear and asperity contact in the mixed-lubrication regime, the interfacial shear stress τ_{is} and asperity contact stress τ_{ac} are given by[12, 17]

$$\left.\begin{aligned}\tau_{is} &= \tau_1 + \tau_2\\ \tau_{ac} &= \tau_0 + \mu_0 p_{ac}\end{aligned}\right\} \tag{15}$$

where τ_1 and τ_2 are the inter-fluid shear stress and shear stress of the fluid acting on bumpy peaks, respectively; τ_0 and μ_0 are the shear stress and boundary friction coefficients, respectively.

The total friction force is then defined by

$$F_f = F_{is} + F_{ac} = \iint \tau_{is}\mathrm{d}x\mathrm{d}y + \iint \tau_{ac}\mathrm{d}x\mathrm{d}y \tag{16}$$

where F_{is} and F_{ac} are the friction forces of the oil film and asperity contact, respectively.

After F_f and W_b are determined, the friction coefficient μ of the CB can be calculated by[18]

$$\mu = \frac{F_f}{W_b} \tag{17}$$

The parameters of W_b, F_f, and μ were selected as evaluation indices to analyze the tribological properties of the CB in this study[12, 18]. Two other parameters, namely, W_{ac} and F_{ac}, were also selected to analyze the influence of the asperity contact on the tribological properties of the CB in the mixed-lubrication regime. Thus, increases in LBC and reductions in the frictional force of the CB could be described by objective functions. The computational scheme for the objective functions is conducted in MATLAB, as shown in Fig. 3.

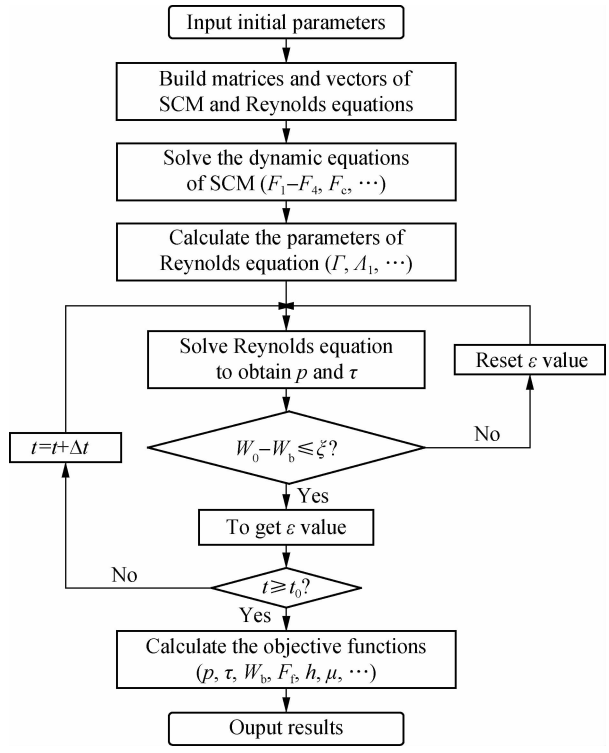

Fig. 3 Computational flowchart

Tab. 1 Simulation parameters

Parameters	Values	Parameters	Values
l/mm	129.5	B/mm	20
r/mm	40	R/mm	36.5
m_p/kg	0.264	r_b/mm	25
m_{cr}/kg	0.345	p_0/Pa	101 325
m_{sr}/kg	0.095	c/μm	10
m_{br}/kg	0.250	η/(Pa·s)	0.02
φ/(°)	720	t_0/(MN·m^{-2})	2
λ	0.309	E^*/GPa	140

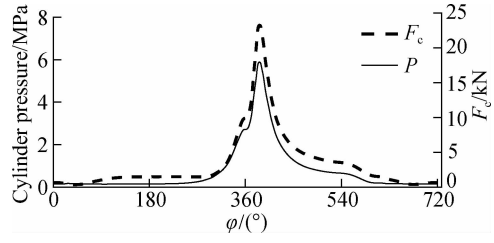

Fig. 4 Dynamic force of the SCM

2 Results and Discussion

The parameters listed in Tab. 1 and the external force $F_c = W_0$ obtained at a crankshaft speed of 2 000 r/min, as indicated in Fig. 4,[4, 15] are applied to highlight the effect of the asperity contact in the mixed-lubrication regime on the tribological properties of the CB. The effects of various radial clearances and surface roughness values on the tribological properties of the CB are then investigated.

2.1 Effect of radial clearance

The effects of different radial clearances of (c = 5, 10, 15, 20, 25 μm) between the shaft and bearing are simulated, and the distribution results of the oil film pressure and shear stress on the CB surface at c = 10 μm are shown in Fig. 5. The results indicate that the highest pressures of the oil film are mainly distributed from 90° to 180° of the circumferential coordinates, and the maximum pressure of the oil film (88.8 MPa) occurs at

158° when the bearing width is $B/2$. The shear stress is uniformly distributed along the bearing width but changes remarkably over the circumferential coordinates evaluated and peaks at 178°.

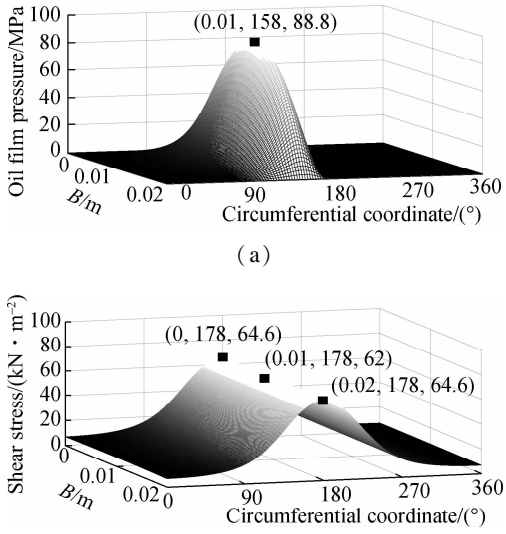

Fig. 5 Pressure and shear stress distributions of the oil film on the bearing surface at $c = 10$ μm. (a) Pressure distributions; (b) Shear stress distributions

The oil film pressure and shear stress distributions obtained at a bearing width of $B/2$ under various radial clearances are illustrated in Fig. 6. Fig. 6(a) shows that the oil film pressure is greatly increased by increasing c. Conversely, the oil film shear stress increases when c is reduced because the micro asperity contact between the bearing and shaft surfaces in the mixed-lubrication regime increases, which, in turn, increases the friction force. The simulation results of the tribological properties are shown in Fig. 7 to clarify the effect of the various radial clearances on the tribological properties of the CB. The results in Figs. 7(a) and (b) indicate that the maximum total load W_b increases whereas the total friction force F_f markedly decreases with increasing c, especially at $c = 25$ μm. The tribological properties of the CB are thus improved.

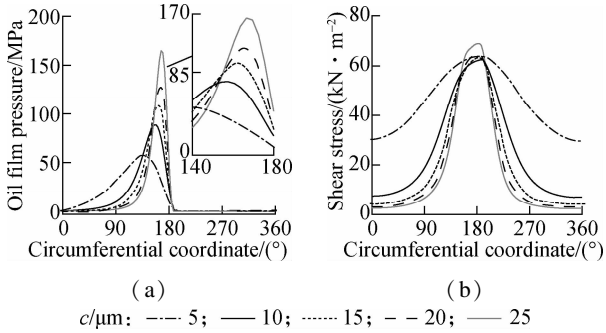

Fig. 6 Oil film pressures and shear stresses obtained at a bearing width of $B/2$ under different radial clearances. (a) Pressure distributions; (b) Shear stress distributions

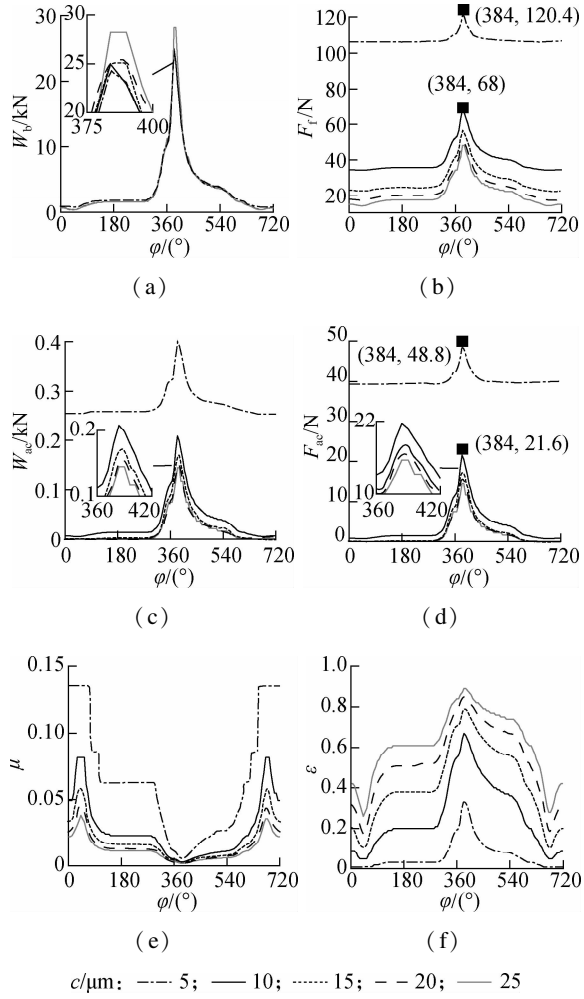

Fig. 7 Effect of the radial clearance of the CB on its tribological properties. (a) Total LBC; (b) Total friction force; (c) LBC of the asperity contact; (d) Friction force of asperity contact; (e) Friction coefficient; (f) Eccentricity ratio ε

The above results indicate that assessing the effect of the micro asperity contact on the tribological properties of the CB under various radial clearances may be challenging. Thus, the effect of the asperity contact region is highlighted by plotting the results of the LBC and friction force of the asperity contact, as shown in Figs. 7(c) and (d). The results indicate that the W_{ac} and F_{ac} of the micro asperity contact increase when c is reduced, especially at $c = 5$ μm. However, W_{ac} is very small in comparison with W_b under the various radial clearances evaluated. Therefore, the LBC of the CB is mainly supported by the oil film, and the radial clearance does not remarkably affect the LBC of the CB. Conversely, as shown in Fig. 7(d), the friction force tends to increase with decreasing c and vice versa. In particular, the maximum F_{ac} accounts for 40.5% and 31.8% of the maximum F_f at $c = 5$ μm and $c = 10$ μm, respectively. Therefore, in addition to the friction force F_{is} of the oil film, the F_{ac} of the asperity contact greatly affects the resistance of the CB.

Under the influence of F_{ac}, the total friction force of F_f

increases remarkably under the various radial clearances. As indicated in Fig. 7(e), the friction coefficient also increases, particularly at $c = 5$ μm. Moreover, as the radial clearance decreases, the eccentricity ratio ε between the shaft and the bearing change minimally, as shown in Fig. 7(f), which improves the stability of the bearing. Although reducing the radial clearance can decrease the eccentricity, an increase in the probability of solid contact will result in a significant increase in friction in the asperity contact region of the CB. In other words, a larger radial clearance can effectively reduce friction. However, an excessively large radial clearance can cause the eccentricity ratio between the shaft and bearing to fluctuate greatly, causing the collision between the shaft and bearing. As the radial clearance gradually increases, the reduction in the friction coefficient becomes very limited. Thus, according to the simulation and analysis results, the optimal radial clearance range providing both anti-friction and anti-impact properties simultaneously is 15 μm $\leqslant c \leqslant$ 20 μm.

2.2 Effect of surface roughness

The effect of the surface roughness of the CB ($\sigma = 2$, 4, 6, 8, and 10 μm) on its tribological properties under the same conditions of a load W_0 at 2 000 r/min is also evaluated. The simulation results of the oil film pressure and shear stress distributions at a bearing width of $B/2$ are shown in Fig. 8. The oil film pressure and shear stress increase with decreasing σ and vice versa. Thus, the surface roughness σ can affect the tribological properties of the CB. This finding is further analyzed by plotting the results of the tribological properties, as shown in Fig. 9.

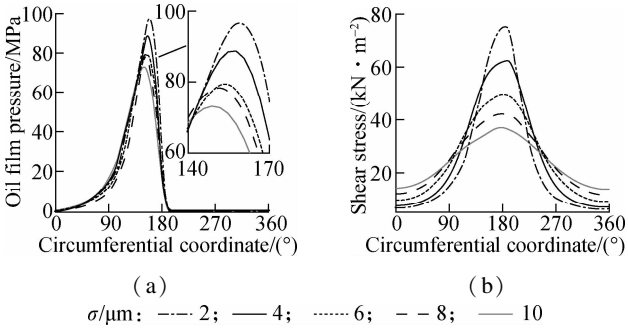

Fig. 8 Oil film pressures and shear stresses obtained at a bearing width of $B/2$ under different surface roughness values. (a) Pressure distribution; (b) Shear stress distribution

Figs. 9(a) and (b) reveal that the maximum W_b is unremarkably affected by the σ while the F_f remarkably increases with increasing σ, especially at $\sigma = 8$ μm and $\sigma = 10$ μm. Figs. 9(c) and (d) demonstrate the influence of surface roughness on the W_{ac} and F_{ac} of the asperity contact. The results show that W_{ac} and F_{ac} significantly increase with increasing σ, which could be explained as follows. As the height of the surface roughness increases, the probability of solid contact in the asperity contact region of the CB surfaces also increases, thereby increasing the pressure and stress of the asperity contact. However, W_{ac} is very small in comparison with W_b under the various surface roughness values tested. Thus, the LBC of the CB depends mostly on the oil film pressure. Conversely, the F_{ac} accounts for a remarkable proportion of the total F_f. In particular, the maximum F_{ac} accounts for 68.3% and 77.7% of the maximum F_f at $\sigma = 8$ μm and $\sigma = 10$ μm, respectively. Thus, the resistance of the CB may be concluded to be greatly affected by the friction force of the asperity contact.

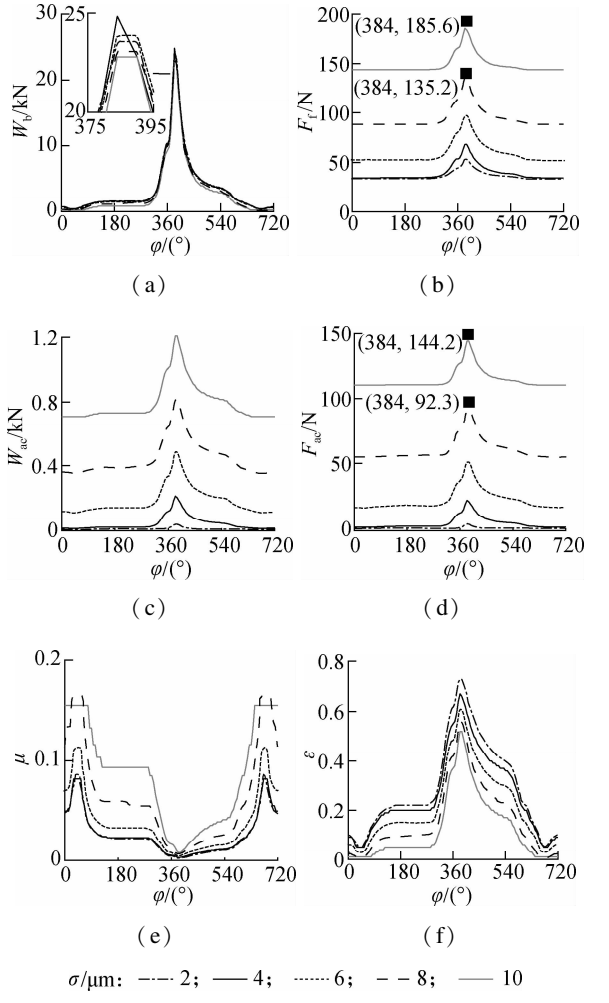

Fig. 9 Effects of surface roughness on the tribological properties of the CB. (a) Total LBC; (b) Total friction force; (c) LBC of asperity contact; (d) Friction force of asperity contact; (e) Friction coefficient; (f) Eccentricity ratio ε

An increase in surface roughness remarkably increases the contact probability between the micro-convex peak and the resistance generated between the solids. Thus, the friction coefficient also increases with F_f, as shown in Fig. 9(e). However, the eccentricity ratio is reduced with increasing σ as shown in Fig. 9(f). An increase in σ causes the p_{ac} in Eq. (12) to increase and the h to decrease. These changes cause a corresponding reduction in

the eccentricity ratio ε in Eq. (6), which means a more stable oil film thickness and shaft rotation.

The tribological properties of the CB are affected not only by its micro asperity contact and radial clearance but also by its speed and dimension[17]. Moreover, the temperature of the oil film can affect the tribological properties of the bearing; thus, the effect of the temperature and viscosity of the oil film on the lubrication performance of the CB must be investigated further.

3 Conclusions

1) The influences of the W_{ac} and F_{ac} of the micro asperity contact on the tribological properties of CBs are analyzed[6, 9]. Results show that the W_{ac} has a negligible influence on the tribological properties of the CB, while the F_{ac} greatly affects its resistance. In particular, the maximum F_{ac} accounts for 40.5% of the maximum F_f at $c = 5$ μm and 77.7% of the maximum F_f at $\sigma = 10$ μm.

2) The W_b significantly increases while the F_f is reduced with increasing radial clearance of the CB. Thus, the tribological properties of the CB are significantly improved. However, an excessively large radial clearance can cause the eccentricity ratio between the shaft and bearing to fluctuate, thereby causing a collision between the shaft and bearing. The results reveal that the optimal radial clearance range providing anti-friction and anti-impact properties simultaneously is 15 μm$\leqslant c \leqslant$20 μm.

3) F_f is strongly decreased, whereas W_b is unremarkably affected when the surface roughness of the CB is reduced. These effects improve the tribological properties of the CB.

4) The numerical simulation method proposed in this study can not only analyze the tribological properties of the dynamic bearing but also correct the design of bearings and optimize design parameters to enhance the tribological properties of CBs.

References

[1] Meng X H, Ning L P, Xie Y B, et al. Effects of the connecting-rod-related design parameters on the piston dynamics and the skirt-liner lubrication[J]. *Proceedings of the Institution of Mechanical Engineers, Part D: Journal of Automobile Engineering*, 2013, **227**(6): 885 - 898. DOI:10.1177/0954407012464025.

[2] He Z P, Gong W Q, Xie W S, et al. NVH and reliability analyses of the engine with different interaction models between the crankshaft and bearing[J]. *Applied Acoustics*, 2016, **101**: 185 - 200. DOI:10.1016/j.apacoust.2015.07.014.

[3] Li Y Y, Chen G P, Sun D Y, et al. Dynamic analysis and optimization design of a planar slider-crank mechanism with flexible components and two clearance joints [J]. *Mechanism and Machine Theory*, 2016, **99**: 37 - 57. DOI:10.1016/j.mechmachtheory.2015.11.018.

[4] Zhao B, Dai X D, Zhang Z N, et al. A new numerical method for piston dynamics and lubrication analysis[J]. *Tribology International*, 2016, **94**: 395 - 408. DOI:10.1016/j.triboint.2015.09.037.

[5] Li Y Y, Chen G P, Sun D Y, et al. Dynamic analysis and optimization design of a planar slider-crank mechanism with flexible components and two clearance joints [J]. *Mechanism and Machine Theory*, 2016, **99**: 37 - 57. DOI:10.1016/j.mechmachtheory.2015.11.018.

[6] Meng X H, Ning L P, Xie Y B, et al. Effects of the connecting-rod-related design parameters on the piston dynamics and the skirt-liner lubrication[J]. *Proceedings of the Institution of Mechanical Engineers, Part D: Journal of Automobile Engineering*, 2013, **227**(6): 885 - 898. DOI:10.1177/0954407012464025.

[7] Jiao R Q, Nguyen V, Van Quynh L, et al. Optimal design of micro-dimples on crankpin bearing surface for improving engine's lubrication and friction[J]. *Industrial Lubrication and Tribology*, 2021, **73**(1): 52 - 59. DOI: 10.1108/ilt-04 - 2020-0152.

[8] Daniel G B, Cavalca K L. Analysis of the dynamics of a slider-crank mechanism with hydrodynamic lubrication in the connecting rod-slider joint clearance[J]. *Mechanism and Machine Theory*, 2011, **46**(10): 1434 - 1452. DOI: 10.1016/j.mechmachtheory.2011.05.007.

[9] Zhao B, Zhang Z N, Fang C C, et al. Modeling and analysis of planar multibody system with mixed lubricated revolute joint[J]. *Tribology International*, 2016, **98**: 229 - 241. DOI:10.1016/j.triboint.2016.02.024.

[10] Zhang H, Hua M, Dong G N, et al. A mixed lubrication model for studying tribological behaviors of surface texturing[J]. *Tribology International*, 2016, **93**: 583 - 592. DOI:10.1016/j.triboint.2015.03.027.

[11] Liu J. A dynamic modelling method of a rotor-roller bearing-housing system with a localized fault including the additional excitation zone[J]. *Journal of Sound and Vibration*, 2020, **469**: 115144. DOI:10.1016/j.jsv.2019.115144.

[12] Zhao B, Zhang Z N, Fang C C, et al. Modeling and analysis of planar multibody system with mixed lubricated revolute joint[J]. *Tribology International*, 2016, **98**: 229 - 241. DOI:10.1016/j.triboint.2016.02.024.

[13] Gropper D, Wang L, Harvey T J. Hydrodynamic lubrication of textured surfaces: A review of modeling techniques and key findings[J]. *Tribology International*, 2016, **94**: 509 - 529. DOI:10.1016/j.triboint.2015.10.009.

[14] Zhang J J, Zhang J G, Rosenkranz A, et al. Surface textures fabricated by laser surface texturing and diamond cutting—influence of texture depth on friction and wear [J]. *Advanced Engineering Materials*, 2018, **20**(4): 1700995. DOI:10.1002/adem.201700995.

[15] Nguyen V, Wu Z P, Van Quynh L. Optimization of crankpin bearing lubrication under dynamic loading considering effect of micro asperity contact[J]. *Industrial Lubrication and Tribology*, 2020, **72**(10): 1173 - 1179. DOI:10.1108/ilt-02 - 2020-0072.

[16] Wang P L, Nguyen V, Wu X Y, et al. Research on different structures of dimpled textures on improving the LEFPL of engine[J]. *Industrial Lubrication and Tribology*, 2021, **73**(4): 545 - 553. DOI:10.1108/ilt-07 - 2020-

0286.

[17] Nguyen V, Zhang J R, Jiao R Q, et al. Research on the effect of crankpin bearing speed and dimension on improving engine power [J]. *Journal of Southeast University (English Edition)*, 2021, **37**(2): 119 - 127. DOI: 10.3969/j. issn. 1003-7985. 2021. 02. 001.

[18] Wu Z P, Nguyen V, Zhang Z H, et al. Study on curved surface design of sliding pair based on stepped topography model[J]. *Industrial Lubrication and Tribology*, 2019, **72**(1): 86 - 92. DOI:10. 1108/ilt-04 - 2019-0121.

微观粗糙接触和径向游隙对曲柄销轴承摩擦性能的影响

阮文廉[1,2,3] 张建润[1] 黄大成[1]

([1]东南大学机械工程学院, 南京 211189)

([2]湖北理工学院机电工程学院,黄石 435003)

([3]湖北理工学院智能输送技术与装备重点实验室,黄石 435003)

摘要:将滑块-曲柄机构(SCM)的动力学模型和曲柄销轴承的润滑模型相结合,开发了一种新的混合模拟方法,以分析微观粗糙接触对曲柄销轴承润滑性能的影响. 在混合模型中,SCM 的动力学方程是基于牛顿法建立的,而曲柄销轴承的润滑方程是根据雷诺方程建立的. 为了提高结果的可靠性,利用发动机的实验数据进行模拟分析,并选择曲柄销轴承的承载能力和摩擦力作为目标函数. 结果表明,在不同的径向间隙和不同的粗糙表面下,曲柄销轴承的承载能力对摩擦性能的影响可忽略不计,而摩擦力极大地影响了曲柄销轴承的阻力. 特别地,粗糙接触区域的最大摩擦力在径向间隙为 5 μm 时占最大总摩擦力的 40. 5%,在曲柄销轴承的粗糙表面 10 μm 处占最大总摩擦力的 77. 7%.

关键词:曲柄销轴承;摩擦性能;曲柄机制;粗糙接触

中图分类号:U461. 3